Supplement of Hydrol. Earth Syst. Sci., 27, 3643–3661, 2023
https://doi.org/10.5194/hess-27-3643-2023-supplement

Hydrology and Earth System Sciences
Open Access
EGU

Supplement of

Accounting for precipitation asymmetry in a multiplicative random cascade disaggregation model

Kaltrina Maloku et al.

Correspondence to: Kaltrina Maloku (kaltrina.maloku@univ-grenoble-alpes.fr)

S1 Fitted models

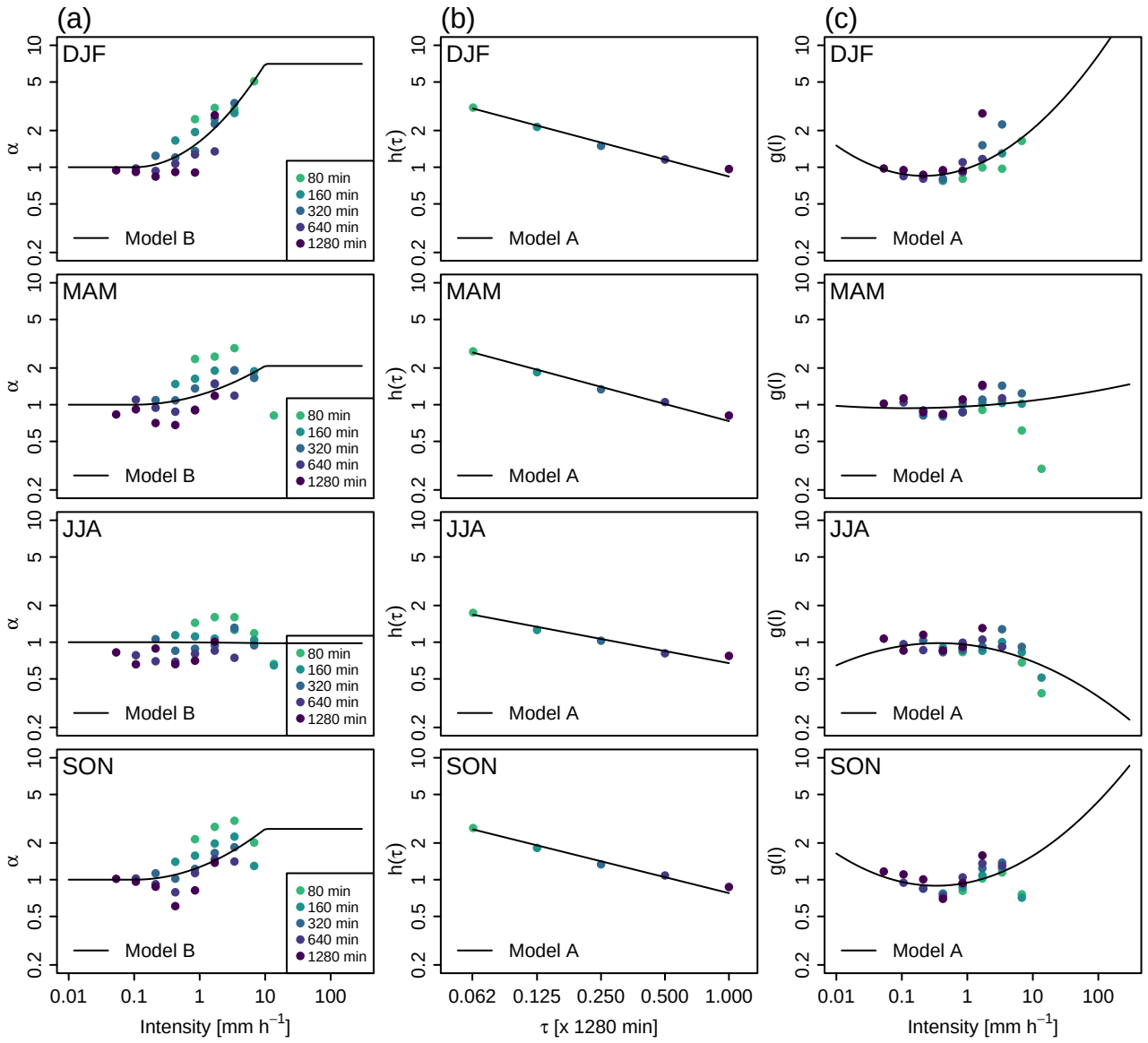

Figure S1. Parameter α of the Beta distribution for f_{W^+}. (a) Estimates α at each temporal scale and intensity class (solid circles) against the intensity and fitted scaling model B, Eq. (13) (solid black line). (b) and (c) the two scaling sub-models for α in model A. (b) Model $h(\tau)$ (Eq. 11) and (b) model $g(I)$ (Eq. 12). See Fig. 1 for caption details. Data from the Zurich station, all seasons.

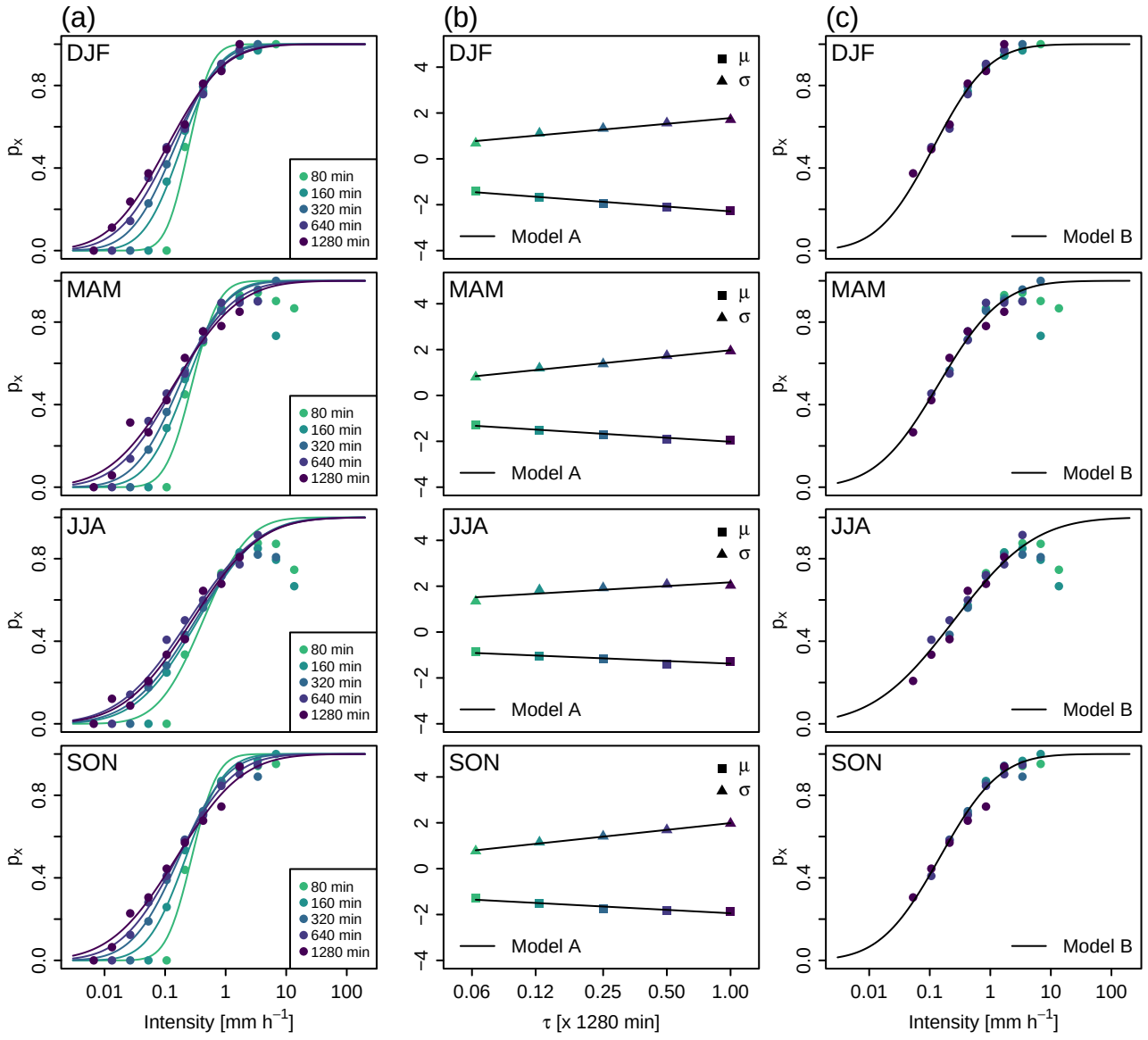

Figure S2. Non-zero subdivisions probability p_x. (a) p_x estimates for different classes of intensity and temporal scale and scaling model $p_x(I,\tau)$ in model A, Eq. (6) . b) Scaling models for the parameters $\mu(\tau)$ and $\sigma(\tau)$ in model A (Eq. 7 and 8, respectively). (c) Scaling model of $p_x(I)$, Eq. (9), in model B (precipitation data below 0.8 mm threshold are disregarded). See Fig. 1 for details.

S2 Performance evaluation

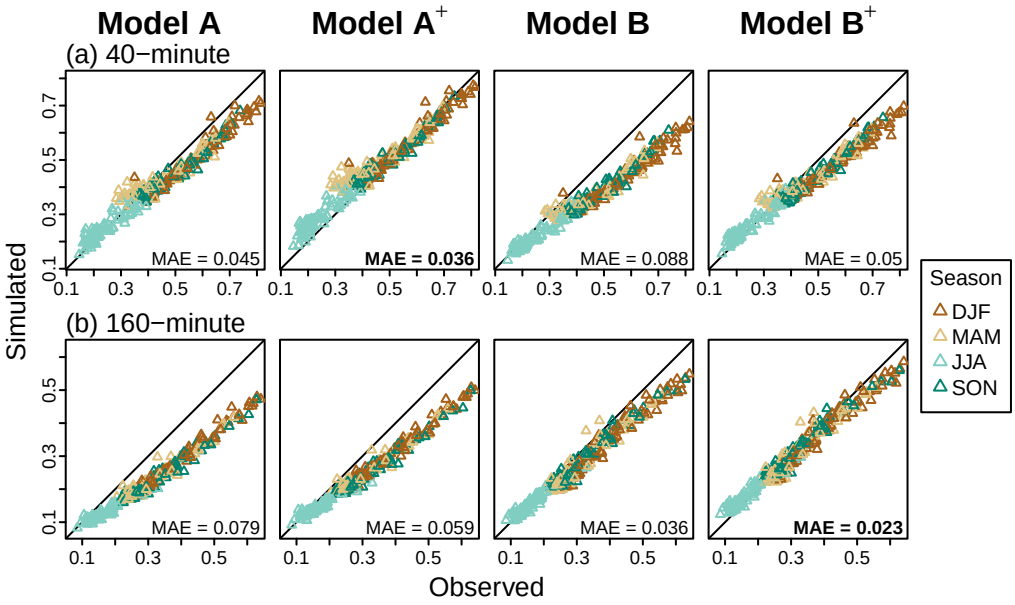

Figure S3. Observed versus simulated lag-2 autocorrelation at (a) 40-minute in resolution (b) and 160-minute resolution. Each triangle represents a site and a season. The triangles for the simulated metrics correspond to the median of the 30 statistics obtained from the corresponding 30 simulated scenarios. MAE values over all sites and seasons are indicated in the bottom-right corner, the lowest MAE obtained over the four models is indicated in bold.

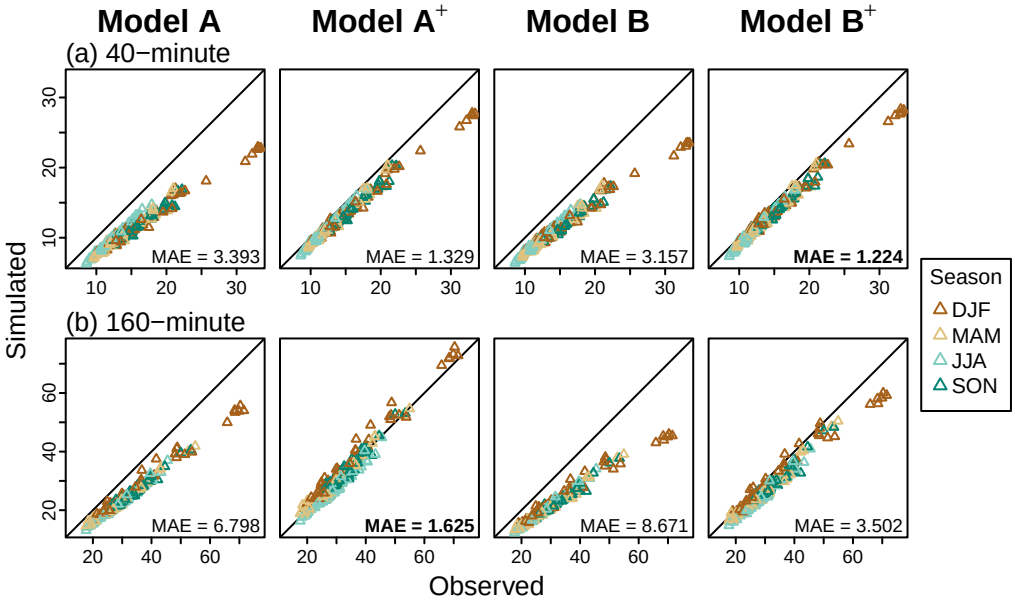

Figure S4. Observed versus simulated mean length of dry spells. Same notation as in Fig. S3.

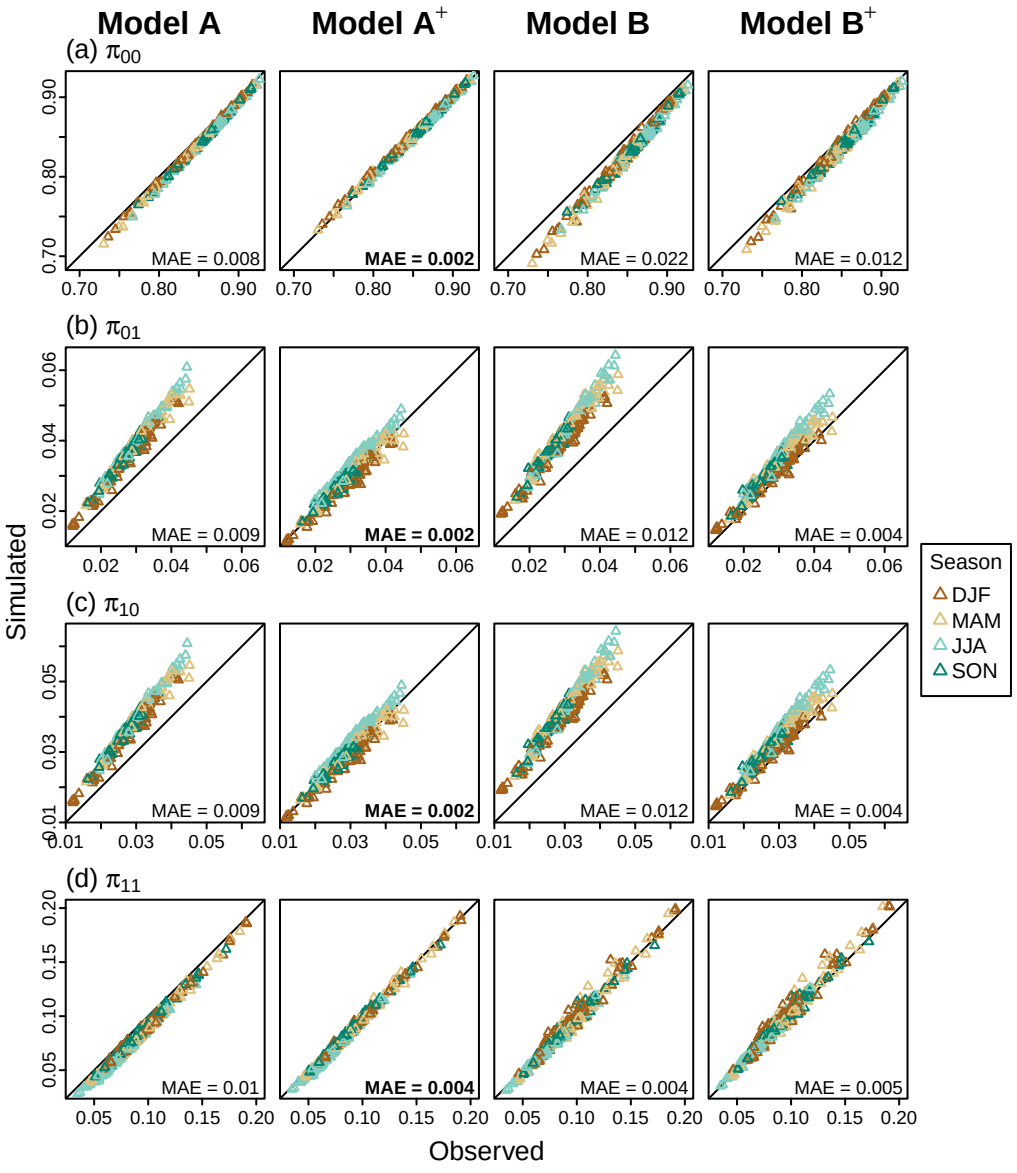

Figure S5. Observed versus simulated transition probabilities at 40-minute resolution at each site for each model. (a) $\pi_{00} = P(R_t = 0, R_{t-1} = 0)$, (b) $\pi_{01} = P(R_{t-1} = 0, R_t = 1)$, (c) $\pi_{10} = P(R_{t-1} = 1, R_t = 0)$ and (d) $\pi_{11} = P(R_{t-1} = 1, R_t = 1)$, where 0 and 1 refer to dry/wet steps respectively. Same notation as in Fig. S3.

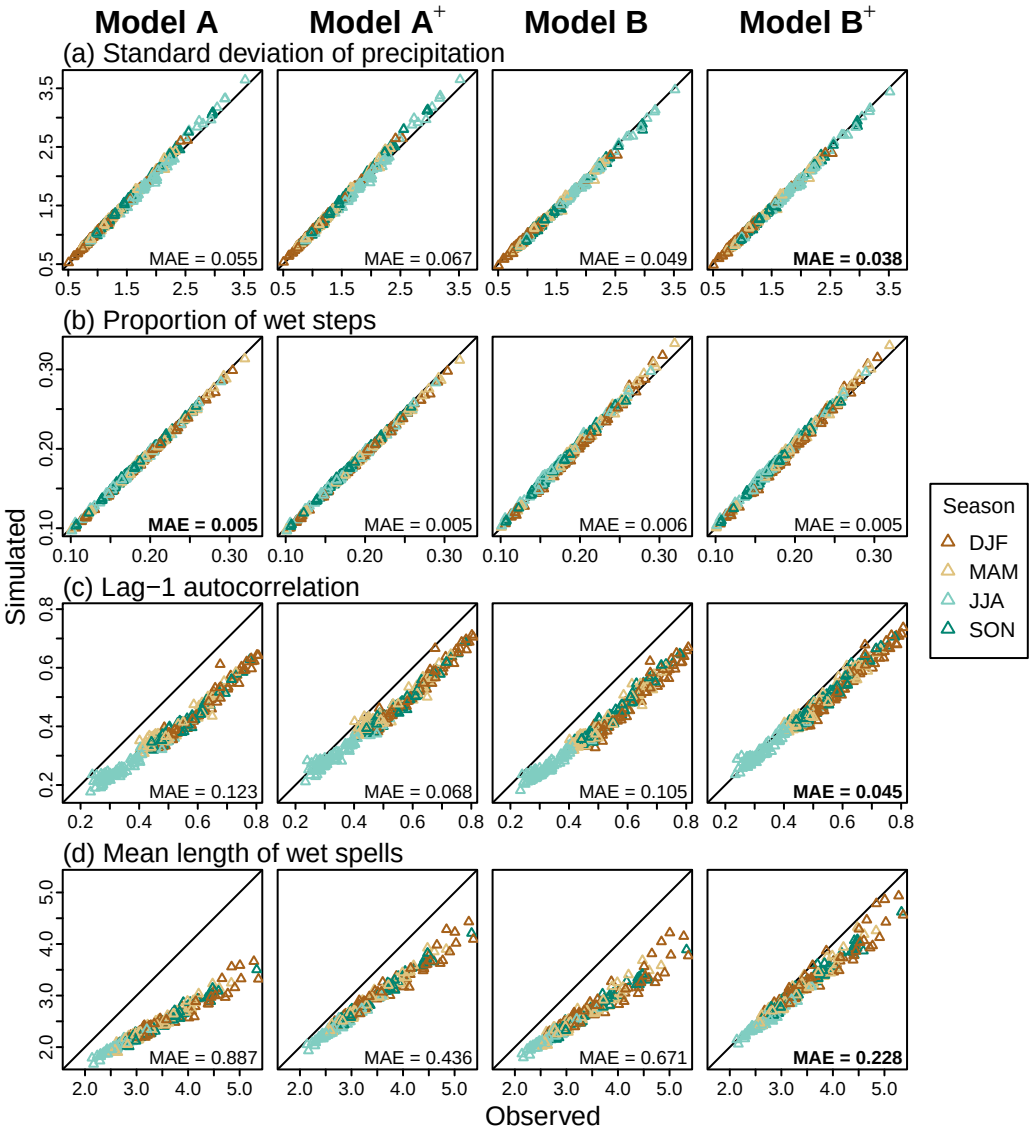

Figure S6. Observed versus simulated statistics for different metrics at 160-minute aggregation level. Same notation as in Fig. S3.

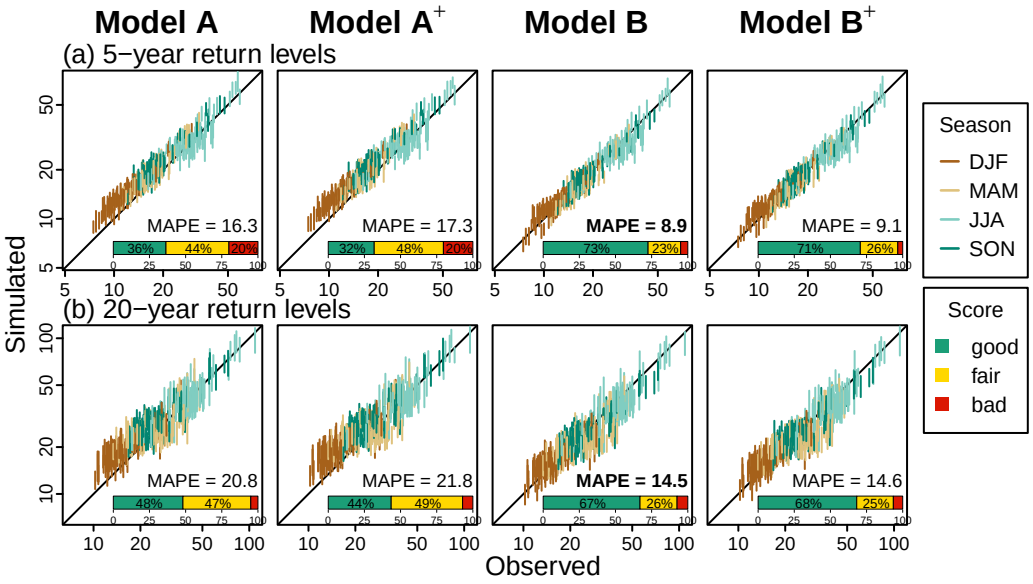

Figure S7. Observed versus simulated return levels at 160-minute temporal resolution for 5- and 20-year return periods, (a) and (b) respectively. Vertical bands indicate the 90% CI limits obtained from the 30 simulated time series for each station and each season (one colour by season). Horizontal coloured bars indicate the percentage of "good", "fair", and "poor" performance as assessed by the CASE framework for all sites and seasons (81 × 4 = 324 cases). The return levels are estimated empirically using the Gringorten plotting position formula (Gringorten, 1963). MAPE values over all sites and seasons are indicated in the bottom-right corner, the lowest MAPE obtained over the four models is indicated in bold.

S2.1 Performance evaluation when seasonal stratification is ignored

The figures below are dedicated to show the importance of seasonal stratification of precipitation data. This time the estimation procedure is performed without distinguishing for seasonality and this way only a set of parameters of obtained for each station. For the sake of comparison with the results when we account for seasonality, the different metrics are estimated on seasonal basis.

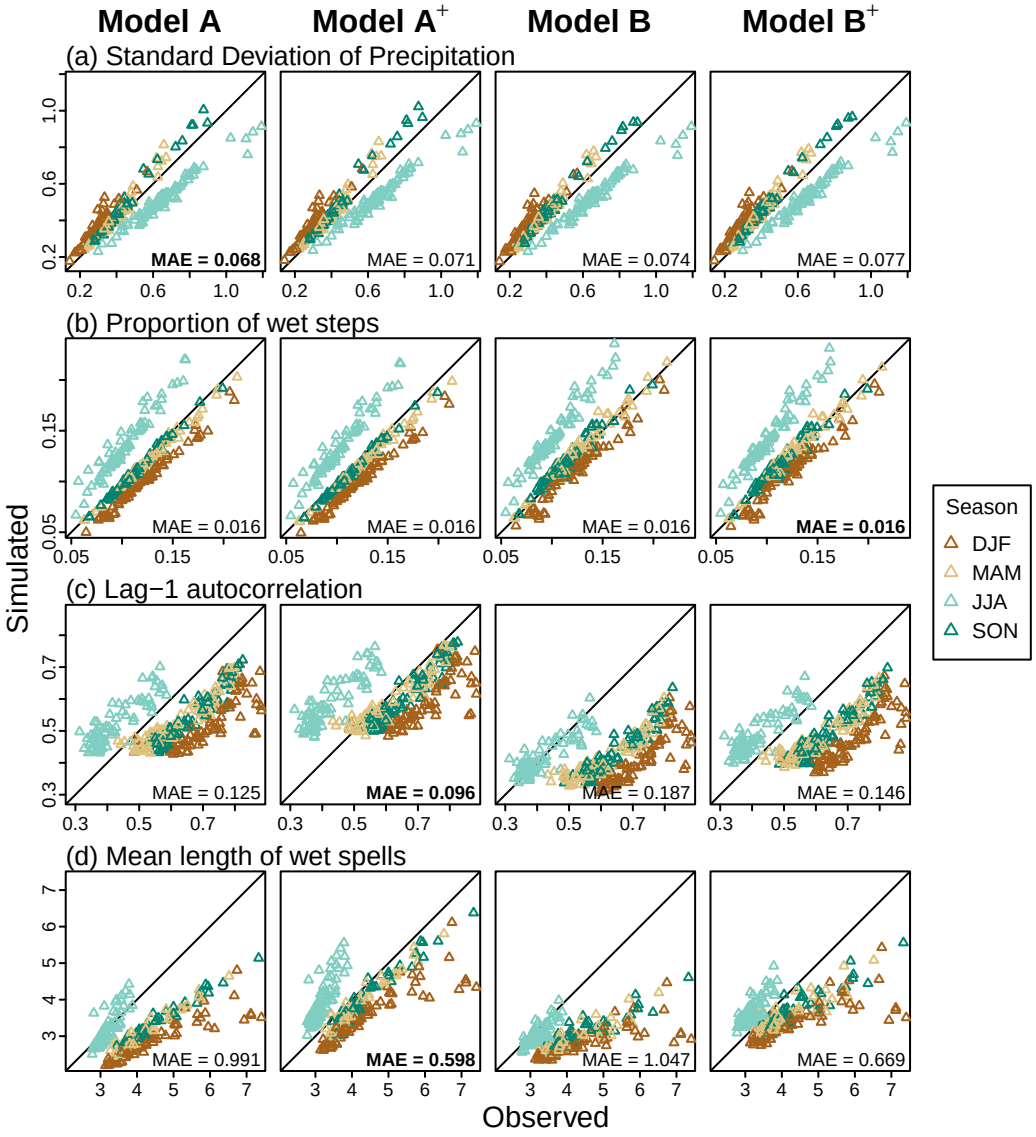

Figure S8. Observed versus simulated statistics for different metrics at 40-minute aggregation level. Seasonal stratification is ignored during the estimation procedure. Same notation as in Fig. S3.

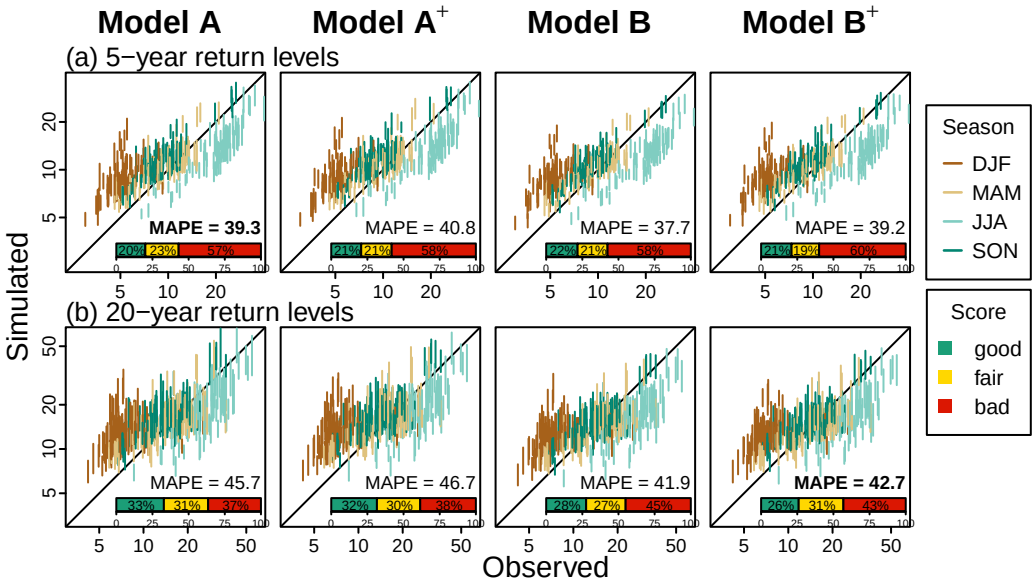

Figure S9. Observed versus simulated return levels at 40-minute temporal resolution for 5- and 20-year return periods, (a) and (b) respectively. Seasonal stratification is ignored during the estimation procedure. See Fig. S7 for details.

S3 Time offset experiment

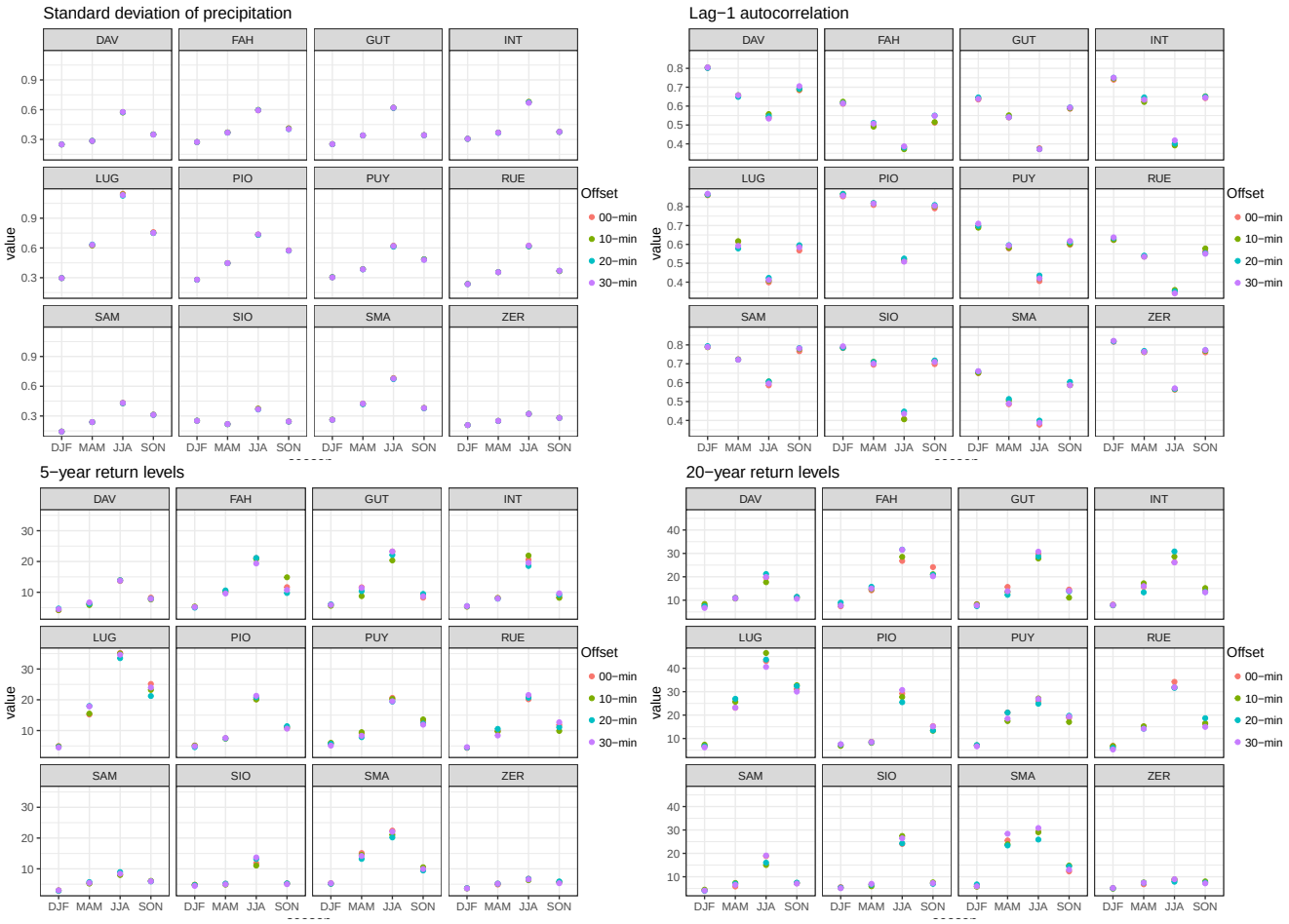

Figure S10. Effect of the offset on observed time series statistics. Observed metrics as estimated on 40-minute time series obtained for different time axis offsets. Top-left is shown the standard deviation, top-right autocorrelation at lag-1, bottom-left return levels for the return period of 5-year and on the bottom-right are shown the results for return levels corresponding to 20-year return period. Each panel corresponds to a given station (results presented for 12 stations).

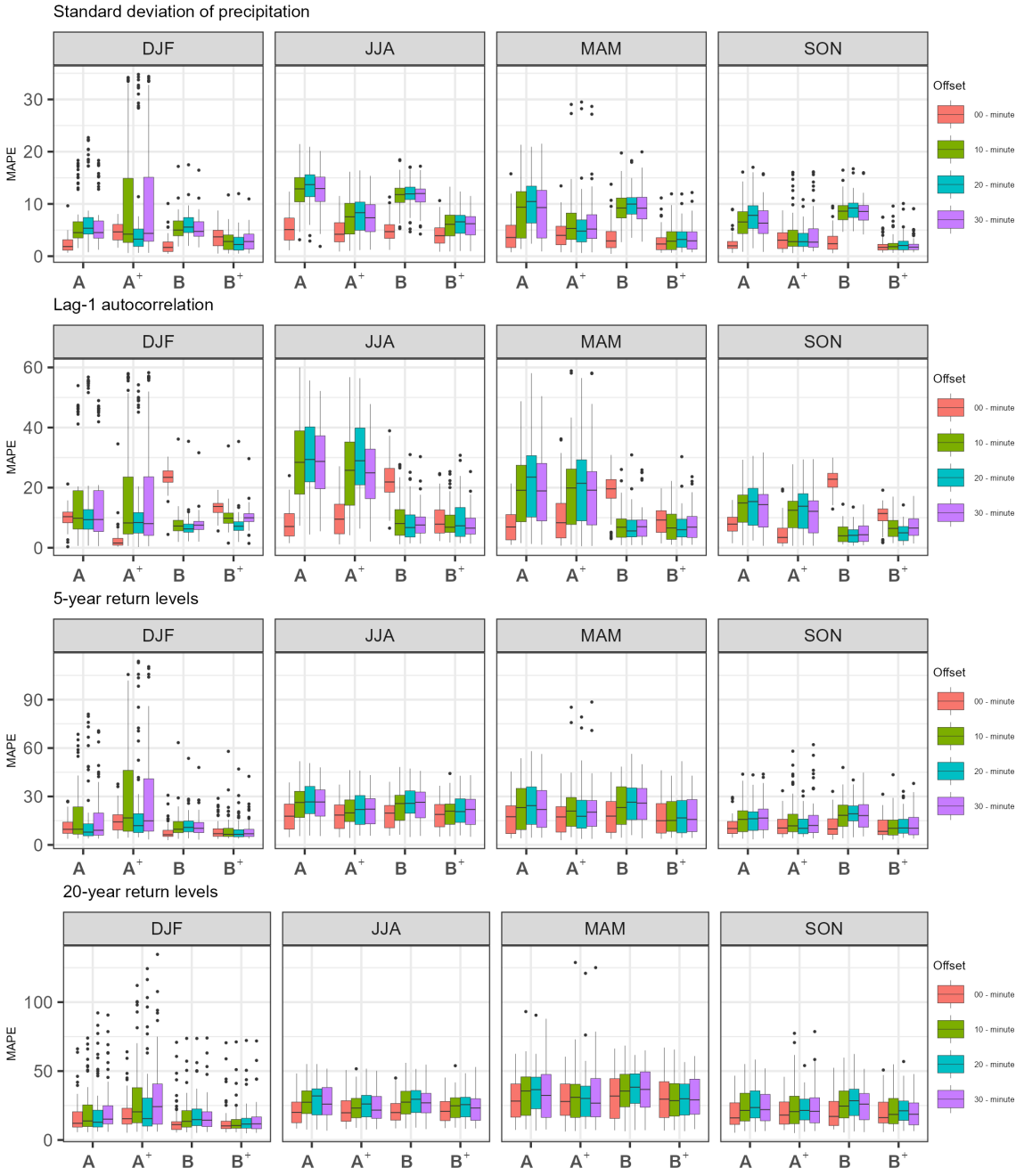

Figure S11. Effect of the offset on disaggregated time series statistics. Mean Absolute Percentage Error (MAPE) between the observed and disaggregated values for different statistics (first row: standard deviation, 2nd row: lag-1 autocorrelation, 3 and 4th row: 5 and 10-year return level). MAPE is given as a function of the time offset (boxplots of different colors: red - no offset, green, blue, purple: 10, 20, 30-minute time offset, respectively), season (DJF, MAM, JJA, SON columns) and disaggregation model (A, A^+, B, B^+). Each boxplot summarizes the single-site performances obtained for 81 stations spread over Switzerland and for the 40-minute temporal aggregation level. Whatever the season, whatever the statistics, the red boxplot (offset 00-min) is very often significantly different from the green/blue/purple boxplots (10, 20, 30-minute).

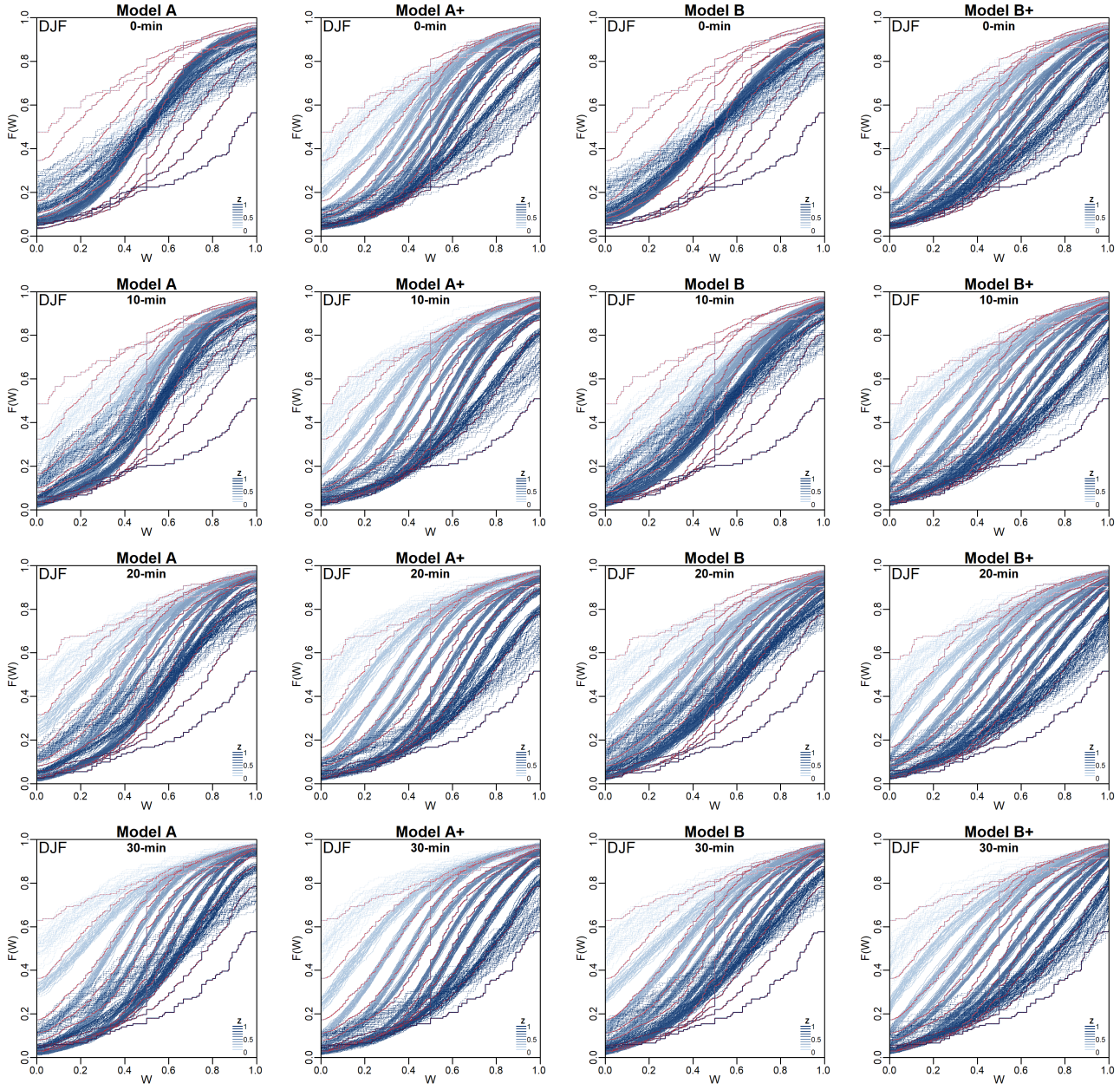

Figure S12. Empirical cumulative distribution functions (ECDFs) of observed and simulated BDCs by the four MRC models (the four columns) and for different time-offsets (first line : no offset, 2nd, 3rd, 4th lines : 10min, 20, min, 30min offsets). The ECDFs are plotted for different classes of the asymmetry index Z as in Figure 3 of the manuscript. The BDC weights are also calculated for precipitation amounts higher than 0.8 mm and the same aggregation levels are considered. Red curves correspond to the ECDFs of observed BDCs. Each shade of blue corresponds to a class of Z-index. The thirty curves of the same shade represent the results from the thirty disaggregated scenarios. The first lines show the ability of the models A+ and B+ to reproduce the dependency of the ECDF to the Z class and the inability of the models A and B to reproduce it. The ECDFs obtained with model A and B are all symmetric, contrary to what is observed. The figure also highlight that the offset-independence property is very well (resp. is not) satisfied when precipitation asymmetry is included (resp. not included) in the MRC. Results for Zurich Data; winter season.

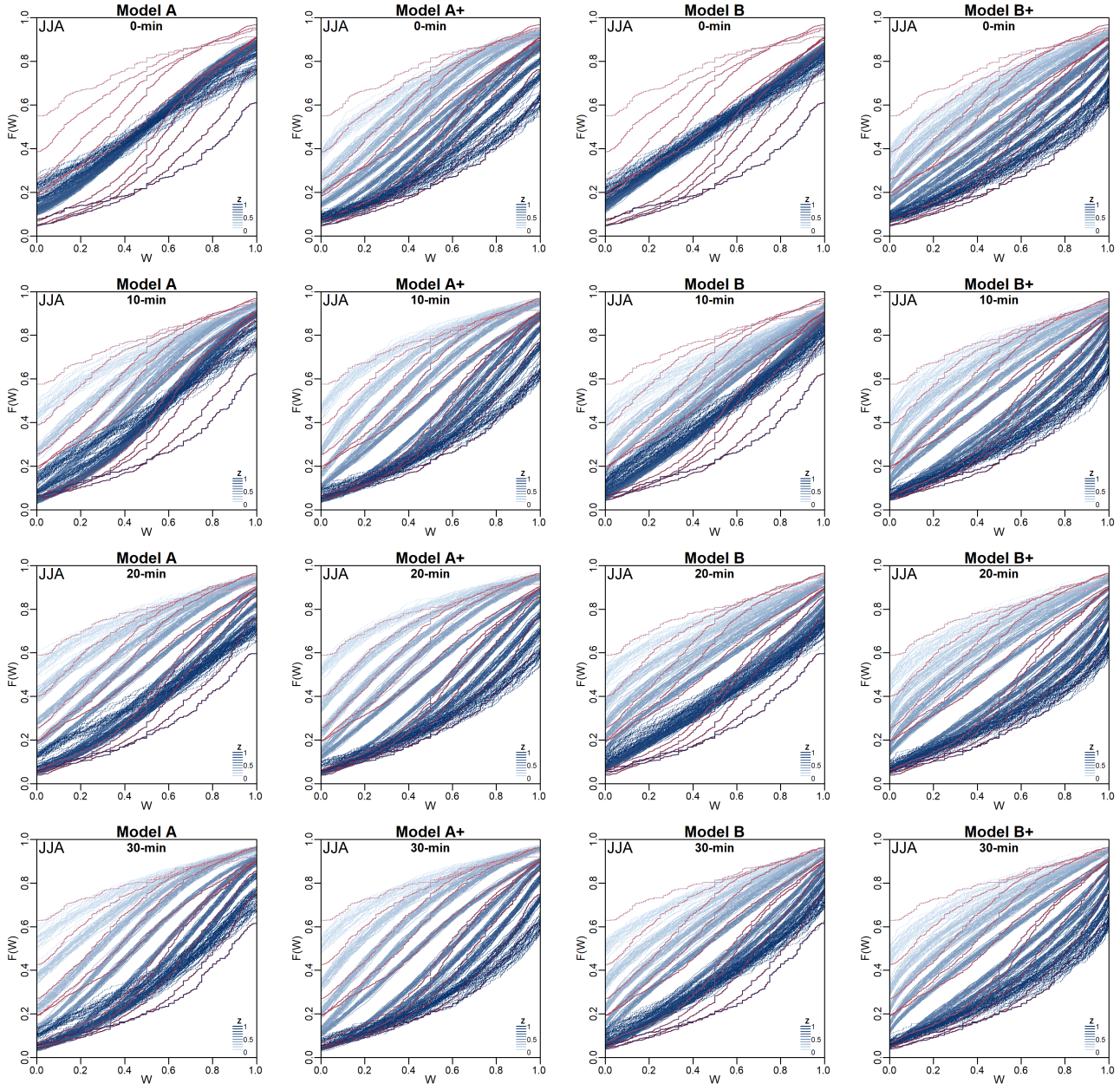

Figure S13. Same caption as Fig. S12 but for summer season.

S4 Conditioning the MRC on ending/starting classes

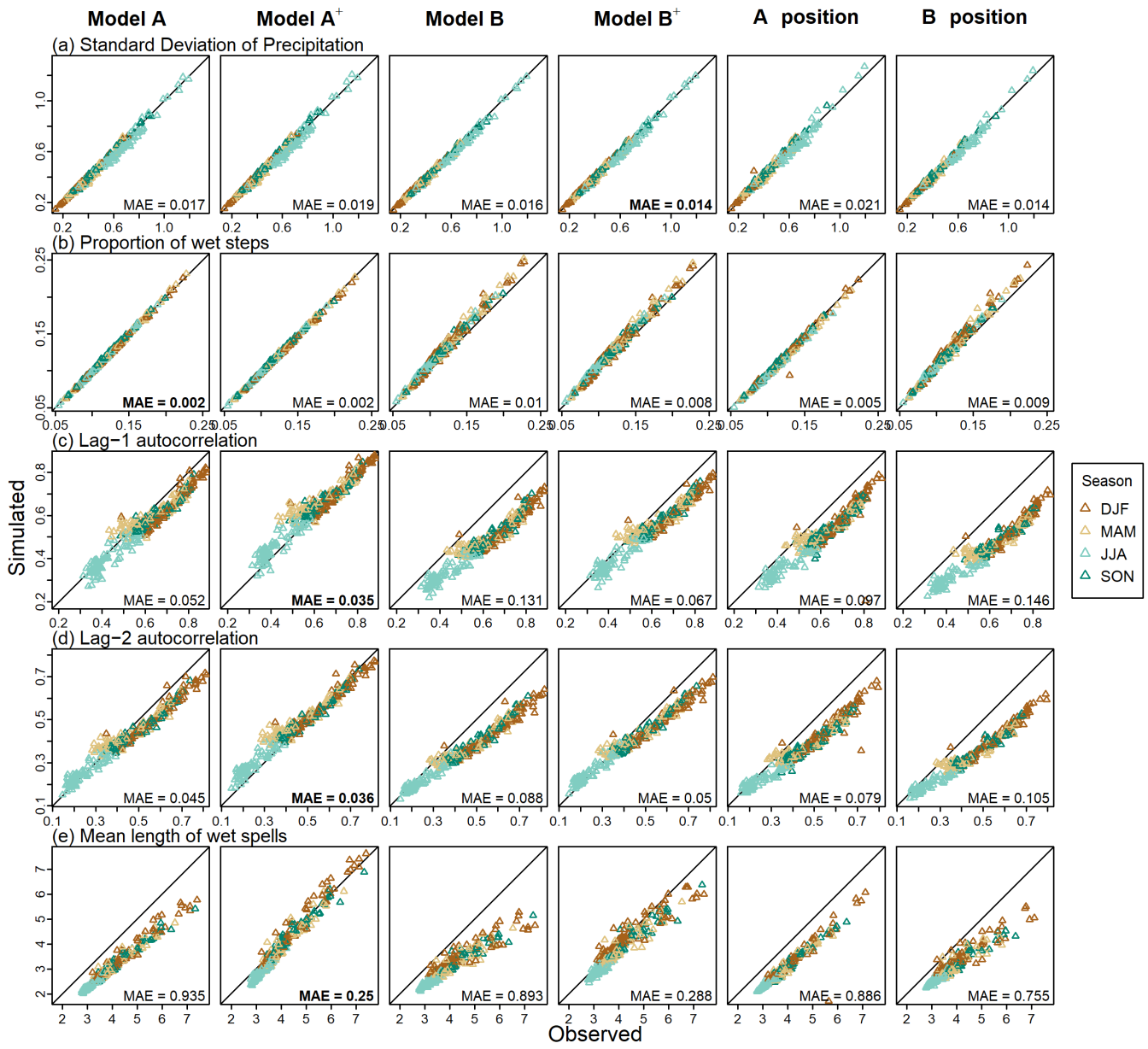

Figure S14. Observed versus simulated statistics for each considered model at a 40-minute temporal resolution for different metrics. Four first columns correspond to the results and models presented in the manuscript, the fifth and sixth column correspond to the results obtained when in the model A, respectively model B, the position class dependency is added.

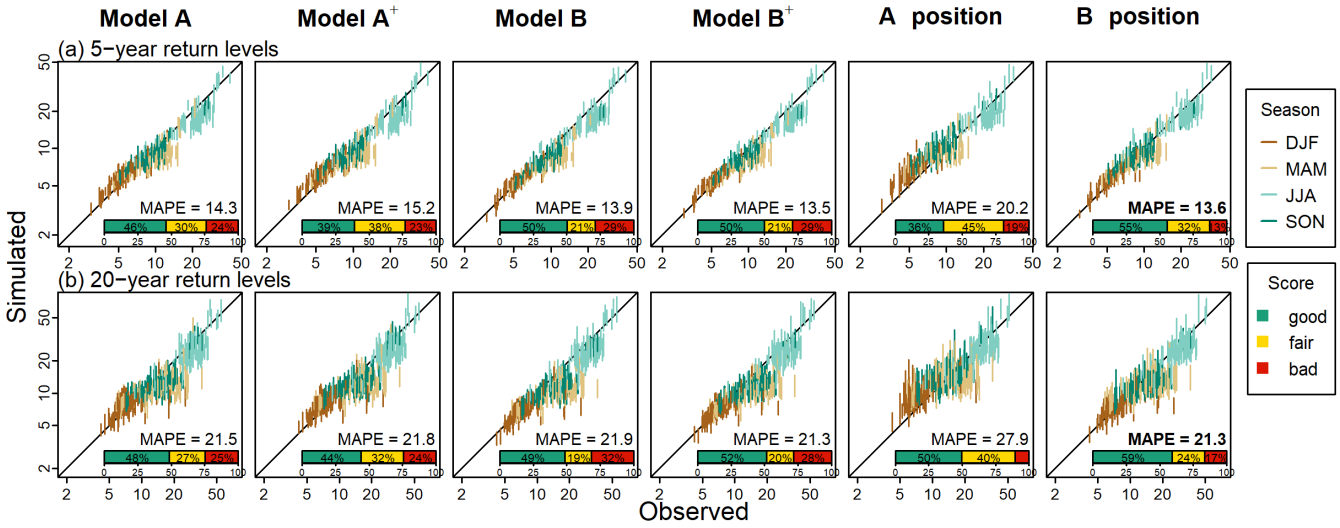

Figure S15. Same notation as in Fig. S14 but different metrics.